Synthesis, Characterization and Bio-Medical, Magnetic Data Storage and Environmental Applications of $Co@SiO_2$ Core/Shell Nanoparticles

J. Alimunnisa*[1], K. Ravichandran[2] and K. S. Meena[1]

[1]*PG and Research Department of Chemistry, Queen Mary's college (A), Chennai-600 004, India*
[2] *Department of Nuclear Physics, University of Madras, Guindy Campus, Chennai 600 025, India*
**Corresponding author email: J. Alimunnisa*

Abstract: **- This paper discusses about the Co core – SiO_2 shell ($Co@SiO_2$) nanoparticles prepared by the modified Stöber method. Phase formation and properties of the particles were studied using X-ray diffraction, field emission scanning electron microscopy (FESEM) with energy dispersive spectroscopy (EDS), X-ray photoelectron spectroscopy (XPS), vibrating sample magnetometer (VSM), impedance spectroscopy (IS), microbial and photo catalytic activities. The insulating layer of SiO_2 shell thickness can block nanoparticles from growing up. Two different phases of cubic structure (f. c. c) for Co and Tetragonal structure of shell SiO_2 were identified from particles. FESEM morphology shows the octahedral symmetric crystal for 0.5 and 1 ml concentration, which is highly porous, well crystallined nature. EDS and XPS measurement peaks show the presence of Co, Si and O elements and confirm the formation of core-shell structure .Paramagnetic for 0.5 ml and diamagnetic behaviour for 1 ml concentration were obtained from VSM measurements. Impedance studies of the sample show very high resistance that is only due to SiO_2 shell. Synthesized nanoparticle having controllable grain size, shape and magnetic property is a suitable candidate for many biomedical, storage, anti-corrosion resistance and environmental applications.**

Key words: **Magnetic nanoparticle, Stöber method, core- shell nanoparticle, XRD, VSM, X- ray photoelectron spectroscopy.**

I. INTRODUCTION

Unique properties small magnetic metal core, oxide shell (core@shell) nanoparticles have recently been grabed the attention of researcher . They have several potential applications in the field of magnetic resonance imaging (MRI) where the ferromagnetism or super paramagnetic properties of the particles provide effective contrast imaging for medical diagnosis, magnetic fluid hyperthermia, controlled drug delivery systems, biosensors, catalysis and energy conversion [1-17]. In physics, ultra high-density magnetic storage medium, an insulating coating around a magnetic nanoparticles (forming a bit – information) improves the reliability and quality of the information being read out. Cobalt NPs have the potential to achieve higher saturated magnetization, that is, three to four times, of iron–oxides. They form non-magnetic cobalt oxides when they are coated with surfactant (such as SiO_2), dramatically increase the resistivity of the bulk material, and remarkably reduce eddy current loss and novel electronic components for spintronics [18–26]. Shell silica plays a major role in the synthesis of core-shell nanoparticle due to excellent physical and chemical properties. Optically transparent, silica surface, which is most frequently used in Stober method synthesis, allows chemically additional functionalization. Magnetic core nanoparticles should be coated with protective layer to prevent them from leaching or coarsening in an acid environment. Cobalt nanoparticle core with dense-coated insulating SiO_2 shell, which can increase the stability of metal nanoparticles and enhance the properties of the metal NPs for a long-time use, and using these kinds of materials, could be a better option in high frequency soft magnetic applications. Each medical application requires materials with different magnetic, thermal, chemical, colloidal stabilities [27-28] and must obviously be non-toxic. Magnetic nanoparticles core/oxide insulating shell can be synthesized by various techniques, but their saturation magnetization is very low [e.g. σ_s = 80 emu/g] [29]. Generally, saturation magnetization materials cannot be directly used in bio or other applications because of oxidation and corrosion characteristics [30].

This paper targets the most famous application of Co/SiO_2 core-shell nanoparticles synthesized by the Stober method and achieved success in cobalt metal core with coating the insulating oxide particles shell. Then, the samples were characterized and extensively studied by XRD, XPS, FESEM with EDS, VSM, Impedance, microbial measurements for the prepared nanoparticles to study its suitability for biomedical, clinical, magnetic data storage and environmental applications.

II. MATERIALS AND METHODS

Reagents

Tetraethoxysilan (TEOS) was purchased from Sigma Aldrich. $AgNO_3$ was obtained from Merck and all the other chemicals used were of Analar grade. Distilled water was used throughout the experiment.

III. EXPERIMENT

Our material was prepared by modified Stöber method as given in literature [9]. It is a one pot process. 5 ml of 0.1 mole

hydrazine solution was blended with 400 ml aqueous solution containing 0.146 gm hexadecyltrymethyl ammonium bromide C_{16}TMABr or $[C_{16}(CH_2)_{15}.N(Br)(CH_3)_3]$ under vigorous stirring for 2 min. In this mixture, hydrazine acts as a reducing agent. Then 10 ml of cobalt (II) nitrate precursor was added drop wise into the solution resulted in the formation Cobalt colloidal particles. While stirring cobalt colloids, 100 ml of ethanol, 4 ml of aqueous ammonia (25 wt %) solution and 0.5 ml of TEOS were added slowly with continuous stirring. The Co@SiO_2 core-shell nanoparticles were separated by centrifugation and washed by ethanol and water for several times. After centrifugation and washing with ethanol and water, the Co@SiO_2 core-shell nanoparticles were obtained.

For the phase formation of synthesized core/shell nanoparticle, X-ray diffraction studies (Seifert 3000P X-ray diffractometer with CuK_α radiation (λ 1.5406 Å) and diffraction reflections were recorded (0.02° with 1 sec counting time in every steps 2 θ scanning range of 20–80°). Morphology was examined using high magnification FESEM with energy dispersive X-ray spectroscopy Hitachi SN6600 model equipped with EDAX. Photoelectron spectroscopy (XPS), $Al_{k\alpha}$ monochromatic X-ray source (Omicron Nanotechnology, UK), was carried out, which confirmed the core/shell structure. Impedance spectroscopy was carried out on a Solartran 1260 model for conductivity study.

IV. RESULTS AND DISCUSSION

The XRD pattern of Co@SiO_2 core/shell nanoparticles shows 0.5 ml (Fig. 1a) 1 ml (Fig. 1b) TEOS samples annealed at 500°C for 19 h. Co peak at 2θ = 44.72°, corresponding to the (111) plane, matched with standard JCPDS data (JCPDS#:894307). The phase was obtained Cubic structure, face-centered lattice, $Fm\bar{3}m$ space group with cell parameter a = 3.544Å. The shell SiO_2 diffraction peaks were at 2θ = 22.05° 31.42°, 36.92°, 59.43°, and 65.18°, corresponding to (101), (102), (112), (114), and (312) planes (JCPDS#:893434), and the phase formation confirmed that Tetragonal structure, Primitive lattice, space group $P4_12_12$, cell parameter a = b = 4.958 Å, c = 6.901 Å.

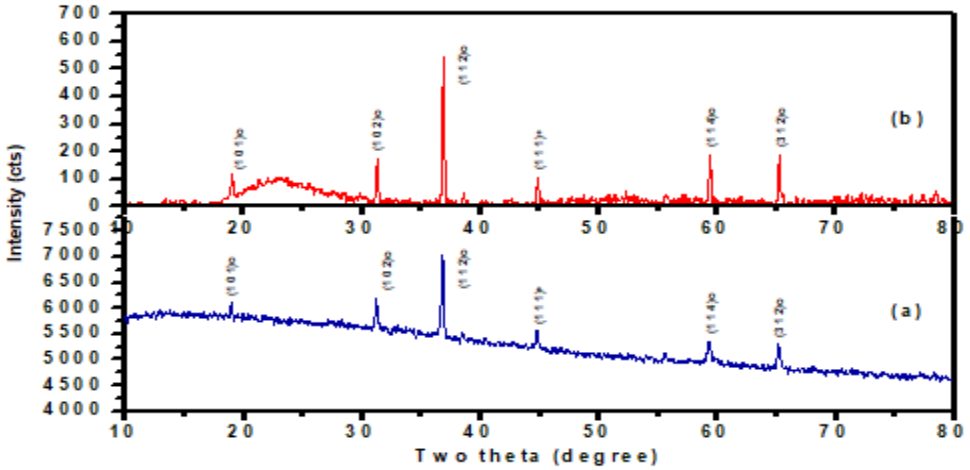

Figure 1 X-ray diffraction results for Co@SiO_2 annealed at 500°C for 19 h samples. (a) 0.5 ml of TEOS concentration, (b) 1 ml of TEOS concentration, annealed at 500°C for 19 h, **(*, °)** Star represent cobalt peak, and open circle represent SiO_2 peak

Using Scherer's formula, the average grain size of the silica-coated cobalt nanoparticles was calculated and was found to be 26.92 nm (Fig. 1a) and 43.77 nm (Fig. 1b).

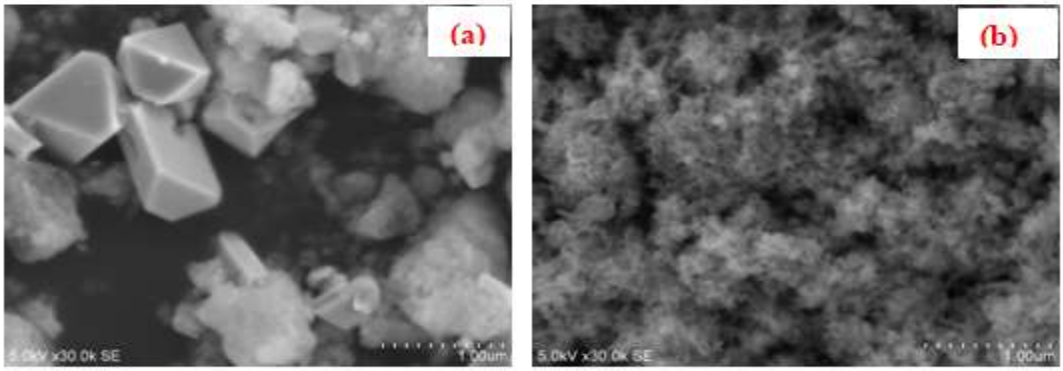

Figure 2. FESEM images of (a) 0.5ml TEOS (b) 1 ml TEOS coated Co@SiO_2

Figure 2a and b shows the FESEM images of 0.5 ml and 1 ml TEOS-coated cobalt. Some crystals of the $Co@SiO_2$ were ordered with low-energy faces (planes). In one case, it showed an octahedral symmetric crystal. FESEM image of $Co@SiO_2$ (1 ml TEOS used) were measured at the same magnification but the morphology obtained was completely different from the former. XRD study reveals that the morphology was highly porous and crystalline.

Figure 3a and b shows the EDAX spectrum of $Co@SiO_2$ excited by an electron beam at 30 kV. The formation of metallic cobalt nanoparticles was confirmed by the energy-dispersive X- ray spectroscopy. The elemental analysis showed the spectrum. Peaks for the Co, Si and O were observed together, and there was no impurity peaks observed in the EDAX spectrum. From EDAX spectra and XRD results, we could confirm the presence of $Co@SiO_2$ core/shell nanoparticles

.Figure 4.1a shows the XPS survey spectrum of $Co@SiO_2$ core/shell (0.5 ml of TEOS coated) nanoparticles. From the survey spectrum, we can confirm the presence of Co, Si, O and C. The high resolution scanning of Co 2p, Si 2p and O 1s peaks were analyzed. It was found that the peak position at 103.4 eV indicates Si^{4+} state bounded with oxygen. Figure 4.1b shows the main peaks at $2p_{3/2}$ = 777.9 eV and 2 $p_{1/2}$ = 792.95 eV corresponding to metallic cobalt. Figure 4.1c shows the XPS of O peaks found at 1s = 531.15 eV and Fig 4.1d shows the XPS peaks of C(1s) for reference binding energy (285 eV) of all measurements**.**

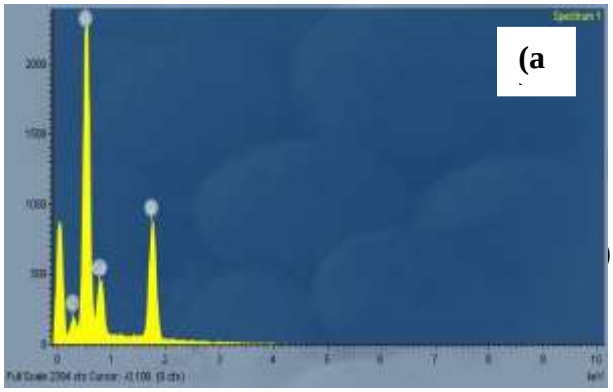

Element	Weight%	Atomic%
C K	4.99	9.16
O K	44.61	61.42
Si K	25.76	20.20
Co L	24.64	9.22
Totals	100.00	100.00

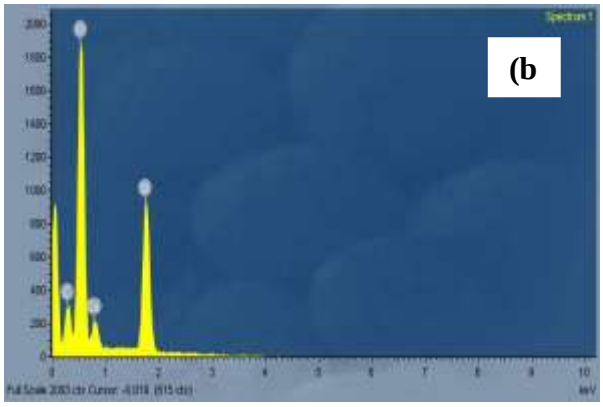

Element	Weight%	Atomic%
C K	10.70	17.55
O K	45.16	55.60
Si K	32.93	23.10
Co L	11.21	3.75
Totals	100.00	100.00

Figure 3 EDAX spectrum of (a) 0.5 ml TEOS, (b) 1ml TEOS coated core- shell

Figure 4.2b shows the high resolution XPS spectrum of Co 2p peaks with the presence of Co bonding with silicate. The peak position was found at 782.0 eV as reported by Jacobsohn *etal.* [12]. XPS and XRD spectra confirm that the prepared material is core-shell nanoparticle.

Figure 5a and b shows the room temperature (RT) hysteresis loop of $Co@SiO_2$ nanoparticles (0.5 ml of TEOS and 1 ml of TEOS concentration). Both are annealed at 500^{o}C for 19 h. Paramagnetic behavior and diamagnetic properties were due to low sensitivity (Fig. 5a and b.). For $Co@SiO_2$ [0.5 ml TEOS] nanoparticles mean coercivity was 327.84 Oe, and the mean retentivity was 0.003391 emu/g [13]. For $Co@ SiO_2$ (1 ml TEOS), the thickness of the shell had increased, which reduced the magnetization

.

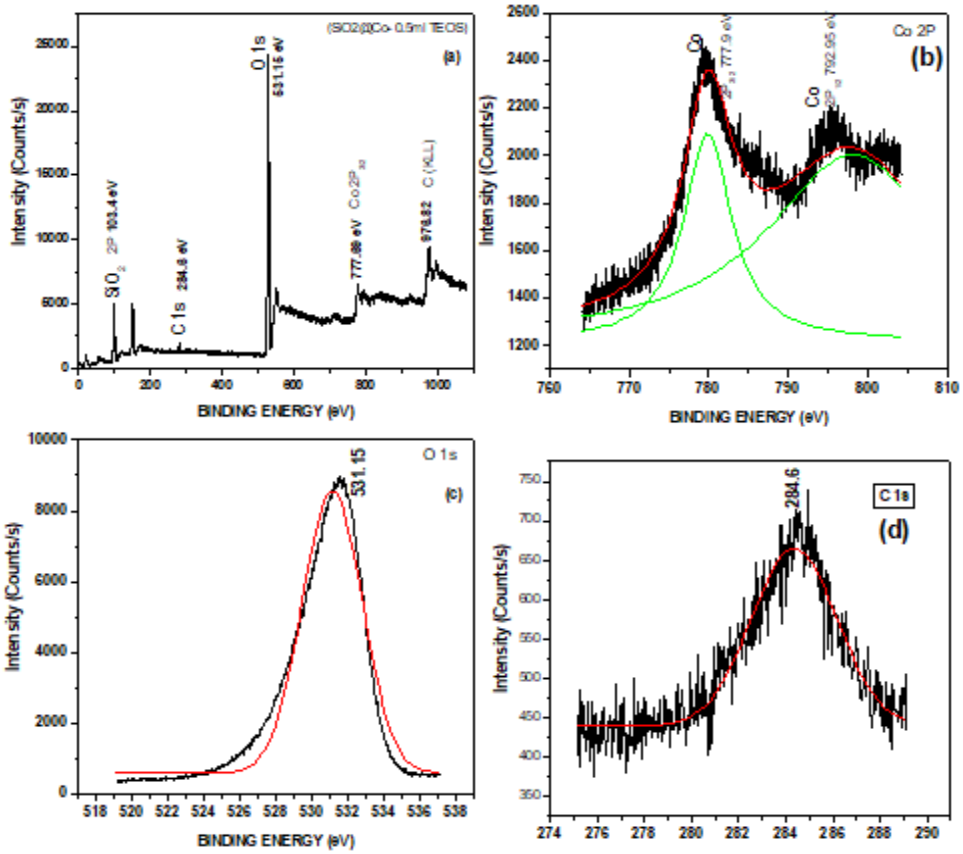

Figure 4.1 XPS spectral line fit (a), Co@SiO_2 Core/Shell (0.5 ml TEOS coated) nanoparticles wide range spectrum (b), Co 2p spectrum (c), O(1s) spectrum and (d) Internal reference C(1s) spectrum. Hint: The spectral curve fitting was performed with OMICRON CASAXPS software version 2.3.

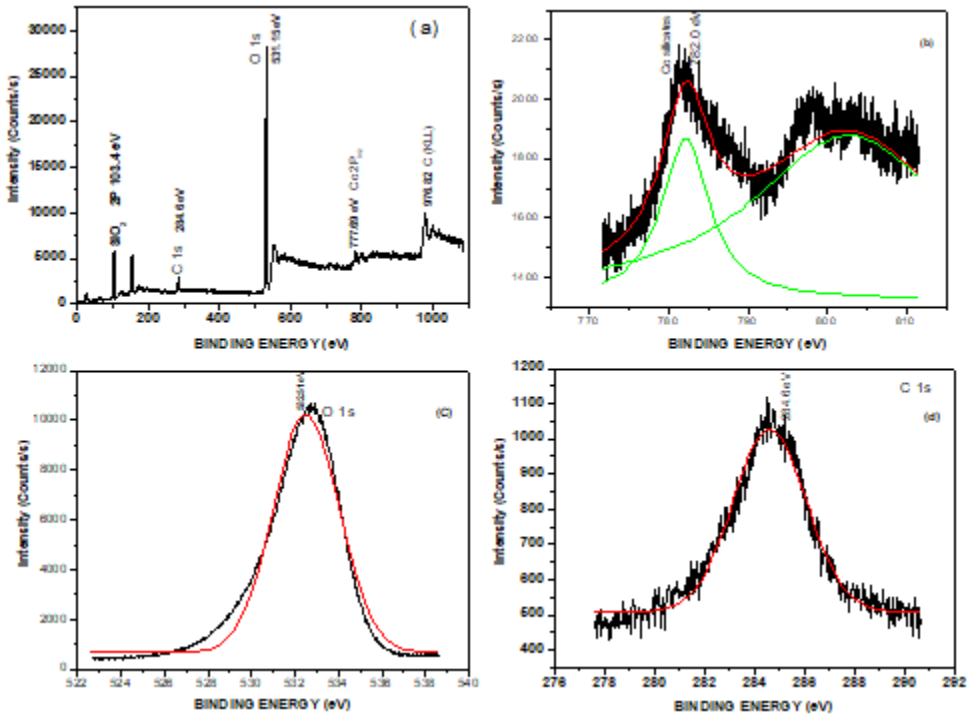

Figure 4.2. XPS spectral line fit (a), Co@SiO_2 Core/Shell (1 ml TEOS coated) nanoparticles wide range spectrum, (b) Co 2P spectrum, (c) O(1s) spectrum, and (d) Internal reference C(1s) spectrum. The spectral curve fitting was performed with OMICRON CASAXPS software version 2.3.

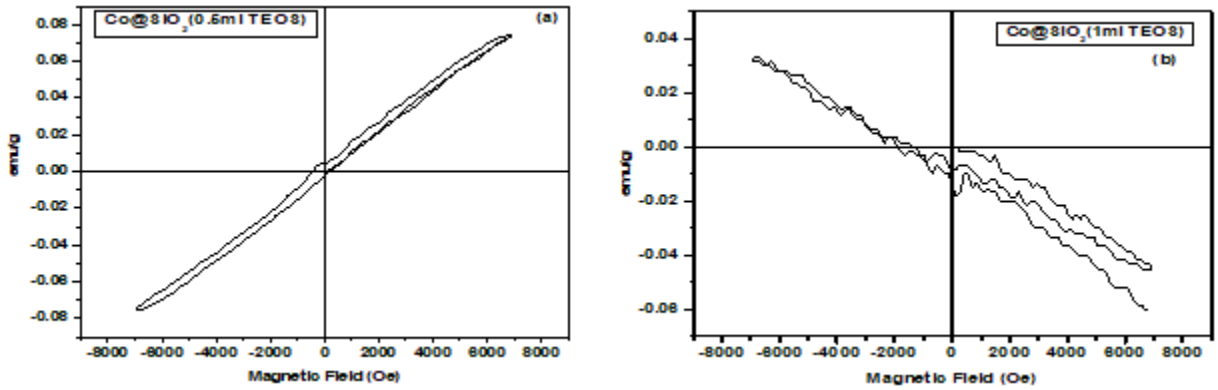

Fig.5. Hysteresis loop for (a) $Co@SiO_2$ core-shell (0.5 ml of TEOS, annealed at 500°C for 19 h, (b) $Co@SiO_2$ core-shell (1 ml of TEOS, annealed at 500°C for 19 h, samples measured at300°K.

Figure 6 shows the impedance analysis of $Co@SiO_2$ (0.5 ml of TEOS) annealed at 500°C for 19 h sample. The impedance measurement was carried out at various temperatures (from RT to 500°C) for $Co@SiO_2$ core/shell nanoparticle annealed at 500°C for 19 h sample. Figure 6a shows typical semi-circular arc behavior at high temperatures. As temperature increased from RT to 500 °C, the radius of the semicircular decreased. It implies the decrease in the resistance of the sample that is due to semiconducting nature of the $Co@SiO_2$. Figure 6b shows the Arrhenius plot of the sample plotted between the reciprocal of the temperature against conductivity. The activation energy corresponding to the temperature-dependent electrical conduction can be estimated using the following expression.

$$\sigma T = \sigma_o e^{(-Ea/kT)}$$

Where σ_o is the pre-exponential factor with dimensions Ω-1 cm-1K, E_a is the activation energy and k is the Boltzmann constant. The Activation energy E_a for the grain conduction in the sample was obtained as 0.0726 eV. Dielectric constant(ε'), Dielectric loss (tan δ) against frequency and temperature in core-shell nanocrystalline $Co@SiO_2$ are plotted as shown in Fig. 6c and d, and are attributed to four types of polarization; interfacial, dipolar, atomic and electronic (or space charge, dipole, ionic and electronic polarization). At lower frequency or lower temperature, all four types of polarization contribute to the dielectric constant and dielectric loss. The gradual decrease in dielectric constant or dielectric loss with frequency in Fig. 6c and d, which is mainly due to interfacial and dipolar polarization.

In the case of dielectric constant, dielectric loss decreased rapidly and became almost constant afterwards (certain frequency or certain temperature). The decrease of dielectric constant and dielectric loss in higher frequency region may be due to the fact that the dipoles cannot follow up the fast variation of the applied field.

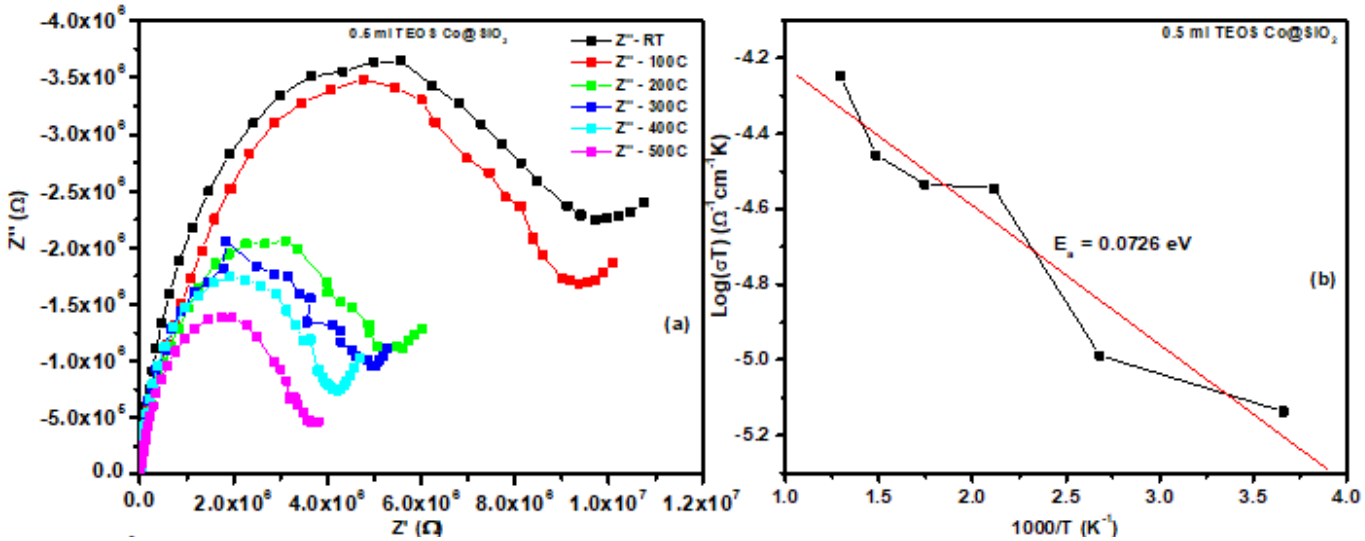

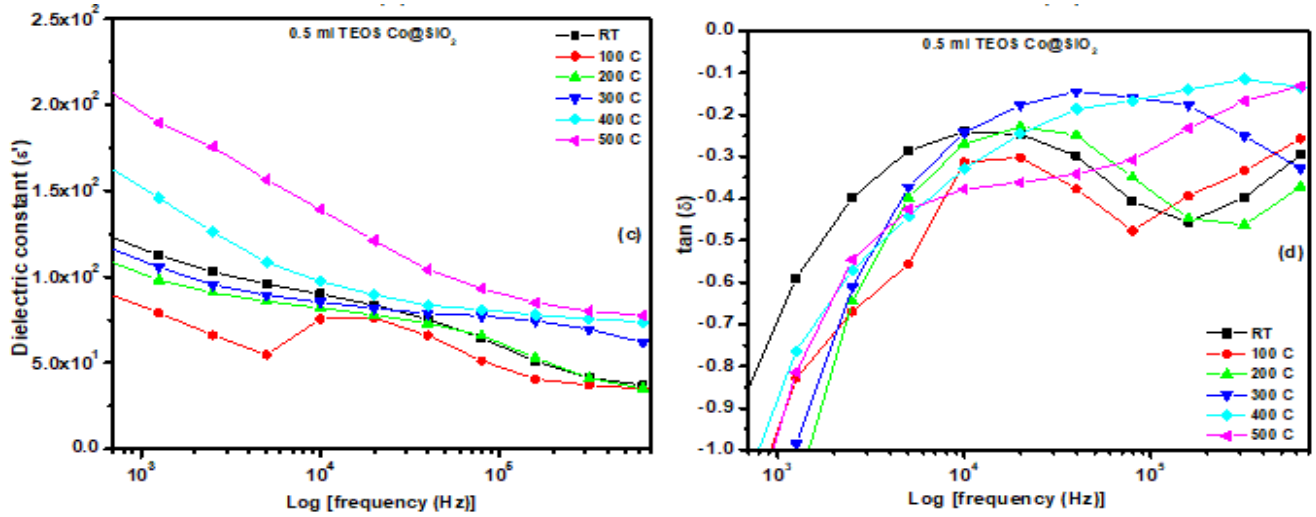

Fig. 6. Impedance plots at high temperatures for nanocrystalline $Co@SiO_2$ (0.5 ml TEOS-coated Co) core/shell sample annealed at 500ºC for 19 h: (a) RT – 500ºC, (b) Arrhenius plot of $Co@SiO_2$ sample, (c) frequency dependence of (Ɛ') and (d) frequency dependence of tan (δ).

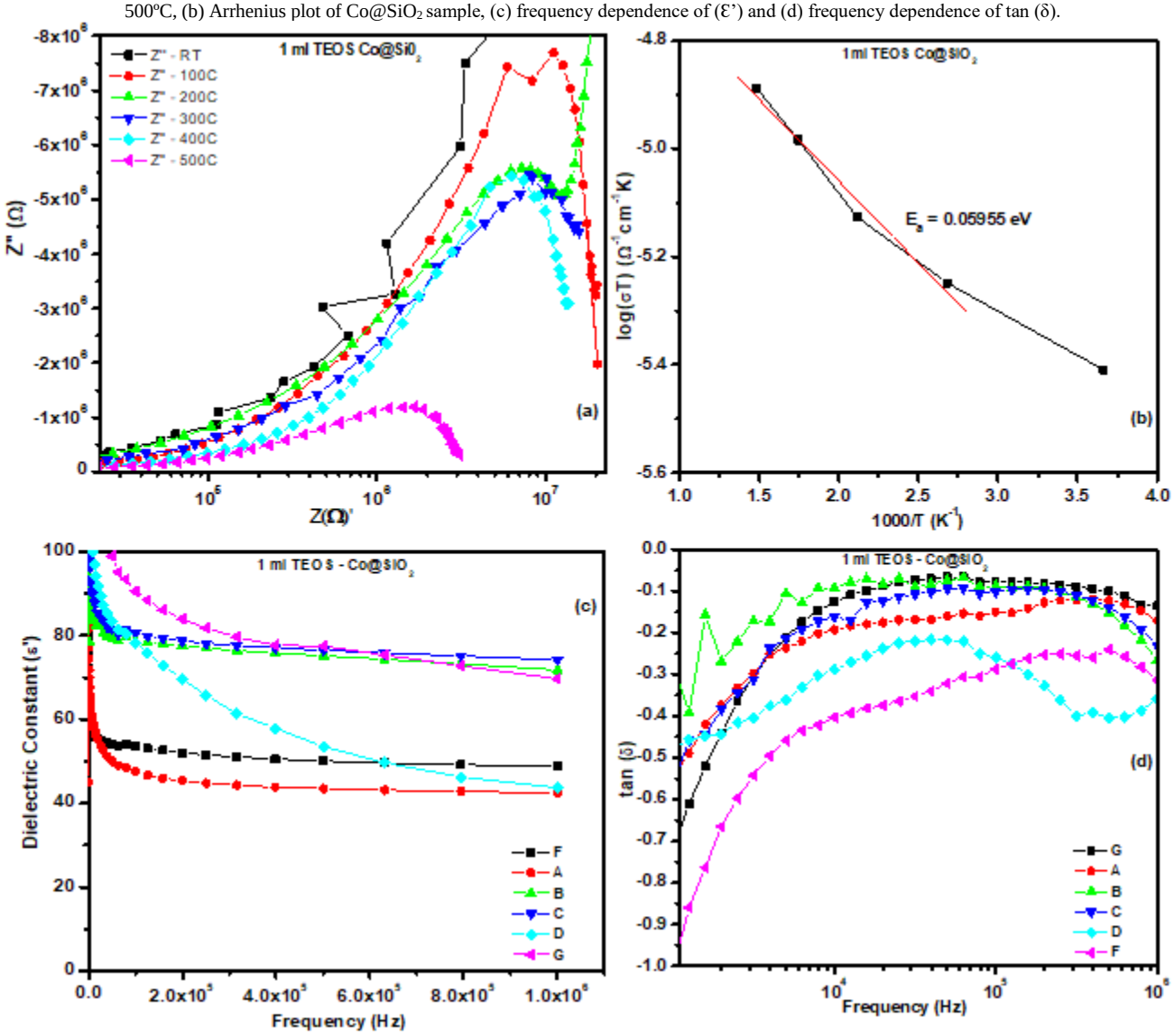

Fig.7. Impedance plots at high temperatures for nanocrystalline $Co@SiO_2$ (1 ml TEOS-coated Co) core/shell sample annealed at 500ºC for 19 h (a) RT – 500ºC, (b) Arrhenius plot of $Co@SiO_2$, (c) frequency dependence of (Ɛ') and (d) frequency dependence of tan (δ).

Impedance analysis of Co@SiO_2 (1 ml of TEOS), annealed at 500°C for 19 h (Fig. 7). The impedance measurement was carried out at various temperatures, from RT to 500^oC, for Co@SiO_2 (1 ml TEOS) core/shell nanoparticle annealed at 500^oC for 19 hours sample. The impedance plots and activation energy are shown in Fig. 7a and b. The activation energy (E_a) was observed 0.05955 eV. Figure 7c and d shows the dielectric constant and dielectric loss plots against frequency or temperature. Gradual increase in frequency or temperature, the dielectric constant and dielectric loss are gradually decreased. Beyond a certain frequency dielectric constant, dielectric loss of the dipoles cannot follow up the fast variation of the applied field.

V. CONCLUSION

Synthesis and characterization of core–shell nanoparticles was performed by modified Stöber method. XRD confirms the crystal structure and the average particle size (26 nm and 43 nm) were calculated. The silica shell thickness was controlled by changing TEOS concentration is responsible for the magnetic property. If the shell thickness increases then the magnetic behavior changes from paramagnetic to diamagnetic. XRD, XPS spectrum confirms the core–shell structure. The activation energy Ea for the grain conduction in the sample was obtained as 0.0726 eV, 0.05955eV.The material has lots of application in storage devices, bio-medical and environmental application because of its biocompatibility in nature.

REFERENCES

[1]. Nagarajan Sounderya and Yong Zhang 2008 Use of Core/Shell Structured Nanoparticles for Biomedical Applications *Recent Patents on Biomedical Engineering* ,1 34-42

[2]. Wagner J, Autenrieth T and Hempelmann R 2002 Core shell particles consisting of cobalt ferrite and silica as model ferrofluids ,*Journal of Magnetism and Magnetic Materials* 252 4-6

[3]. Connolly J, St Pierre T G, Rutnakornpituk M and Riffle J S 2002 Silica coating of cobal nanoparticles increases their magnetic and chemical stability for biomedical applications Eur. Cells Mater. 3 106–9

[4]. Cowburn R.P, 2002 Magnetic nanodots for device applications, Journal of Magnetism and Magnetic Materials 242–245, pp.505–511

[5]. Shouheng Sun, C. B. Murray, Dieter Weller, Liesl Folks, Andreas Moser, 17 Mar 2000, Monodisperse FePt Nanoparticles and Ferromagnetic FePt Nanocrystal Superlattices, *Science* Vol. 287, Issue 5460, pp. 1989-1992

[6]. Y. D. Zhang, S. H. Wang, D. T. Xiao, J. I. Budnick, and W. A. Hines, JULY 2001, Nanocomposite Co/SiO2Soft Magnetic Materials, IEEE Transactions On Magnetics, Vol. 37, No. 4, 2275

[7]. Rodrigues E L and Bueno J M C 2002 Co/SiO2 catalysts for selective hydrogenation of crotonaldehyde II: influence of the Co surface structure on selectivity, *Applied Catalysis A: General* 232 147-58

[8]. Connolly J, Pierre T G S, Rutnakornpituk M and Riffle J S 2004 Cobalt nanoparticles formed in polysiloxane copolymer micelles: effect of production methods on magnetic properties *Journal of Physics D: Applied Physics* **37** 2475-82

[9]. Mehta R V, Upadhyay R V, Charles S W and Ramchand C N 1997 Direct binding of protein to magnetic particles *Biotechnology Techniques* 11 493-6 .

[10]. Pedro Tartaj, Mar´ıa del Puerto Morales, Sabino Veintemillas-Verdaguer, Teresita Gonzalez-Carre´ no and Carlos J Serna, 2003, The preparation of magnetic nanoparticles for applications in biomedicine, J. Phys. D: Appl. Phys. 36 R182-R

[11]. Weissleder R, Stark DD, Engelstad BL, Bacon BR, Compton CC, White DL, Jacobs P, Lewis J. 1989, Superparamagnetic iron oxide: pharmacokinetics and toxicity. AJR Am J Roentgenol. Jan;152(1):167-73

[12]. Muller RH, Maaen S, Weyhers H, et al. 1996. Cytotoxicity of magnetiteloaded polylactide, polylactide/glycolide particles and solid lipid nanoparticles. Int J Pharm, 138:85–94.

[13]. F. Hache, D. Ricard, C. Flytzanis, and U. Kreibig, (1988) "The Optical Kerr Effect in Small Metal Particles and Metal Colloids: The Case of Gold," Appl. Phys., A Mater. Sci. Process. 47(4), 347–357.

[14]. Yin X J, Peng K, Hu A P, Zhou L P, Chen J H and Du Y W 2009 Preparation and characterization of core-shell structured Co/SiO2 nanosphere *Journal of Alloys and Compounds* 479 372-5 (11)

[15]. Lu X, Liang G, Sun Z and Zhang W 2005 Ferromagnetic Co/SiO2 core/shell structured nanoparticles prepared by a novel aqueous solution method *Materials Science and Engineering: B* **117** 147-52 (12)

[16]. Anand C, Srinivasu P, Mane G P, Talapaneni S N, Benzigar M R, Vishnu Priya S, Al-deyab S S, Sugi Y and Vinu A Direct synthesis and characterization of highly ordered cobalt substituted KIT-5 with 3D nanocages for cyclohexene epoxidation *Microporous and Mesoporous Materials* **167** 146-54, Volume 167, February 2013, Pages 146-154 .

[17]. Zhang X, Wei Z, Guo Q and Tian H, 1stJune 2013, Kinetics of sodium borohydride hydrolysis catalyzed via carbon nanosheets supported Zr/Co *Journal of Power Sources* **231** 190-6 .

[18]. Skumryev V, Stoyanov S, Zhang Y, Hadjipanayis G, Givord D and Nogues J, Beating the superparamagnetic limit with exchange bias, Nature Vol.423. No.9, June 2003, pp.850-853.

[19]. Caruso F, Nanoengineering of Particle Surfaces, Advanced Materials, 2001, Vol.13, No.1, pp.11-22.

[20]. Zhong C J, and Maye M M, Core–Shell Assembled Nanoparticles as Catalysts Advanced Materials, 2001, Vol.13, No.19, pp.1507-1511.

[21]. Lyon J L, Fleming D A, Stone M B, Schiffer P, and Williams M E, Synthesis of Fe Oxide Core/Au Shell Nanoparticles by Iterative Hydroxylamine Seeding, Nano Letters, 2004, Vol.4, No.4, pp.719-723.

[22]. Gupta P K, and Hung C T, Magnetically controlled targeted micro-carrier systems, Life Sciences, 1989, Vol.44, pp.175-186.

[23]. Chouly C, Pouliquen D, Lucet I, Jeune J J, and Jallet P, Development of superparamagnetic nanoparticles for MRI: effect of particle size, charge and surface nature on biodistribution, Journal of Microencapsulation, 1996, Vol.13, pp.245-55.

[24]. Weissleder R, Bogdanov A, Neuwelt E A, and Papisov M, Long-circulating iron oxides for MR imaging, Advanced Drug Delivery Reviews, 1995, Vol.16, pp.321-334.

[25]. Mornet S, Lambert O, Duguet E, and Brisson A, The Formation of Supported Lipid Bilayers on Silica Nanoparticles Revealed by Cryoelectron Microscopy, Nano Letters, 2005, Vol.5, No.2, pp.281-285.

[26]. Finotelli P V, Morales M A, Rocha-Leão M H, Baggio-Saitovitch E M, and Rossi A M, Magnetic studies of iron(III) nanoparticles in alginate polymer for drug delivery applications, Materials Science and Engineering: C, 2004, Vol.24, pp.625-629.

[27]. Gu H, Xu K, Xu C, and Xu B, Biofunctional magnetic nanoparticles for protein separation and pathogen detection, Chemical Communications, 2006, pp.941-949.

[28]. Dobson J, Magnetic nanoparticles for drug delivery, Drug Development Research, 2006, Vol.67, pp.55-60.

[29]. Bansmann J, Baker S H, Binns C, Blackman J A, Bucher J P, Dorantes-Dávila J, Dupuis V, Favre L, Kechrakos D, Kleibert A, Meiwes-Broer K H, Pastor G M, Perez A, Toulemonde O, Trohidou K N, Tuaillon J, and Xie Y, Magnetic and structural properties of isolated and assembled clusters, Surface Science Reports, 2005, Vol.56, pp.189-275.

[30]. Shukla R, Bansal V, Choudhury M, Basu A, Bhonde R R, and Sastry M, Biocompatibility of Gold Nanoparticles and Their Endocytotic Fate Inside the Cellular Compartment: A Microscopic Overview, Longmuir, 2005, Vol.21, pp.10644-10654.